Origin of depolarization dispersion of totally symmetric fundamental transitions in the resonance Raman effect of soluble *cis*-polyacetylene

Paola Sassi
Department of Chemistry, University of Perugia, Via Elce di Sotto 8, I-6100 Perugia, Italy

Marek Pawlikowski
Department of Theoretical Chemistry, Jagiellonian University, 30-060 Crakow, Poland

Rosario Sergio Cataliotti
Department of Chemistry, University of Perugia, Via Elce di Sotto 8, I-6100 Perugia, Italy
(Received 23 July 1993; revised manuscript received 6 May 1994)

Two models are presented which we have used to reproduce experimental data, such as Raman excitation profiles and the dispersion of the depolarization ratio of totally symmetric fundamentals, in the excitation range of resonance Raman scattering of *cis*-polyacetylene. The first model works in the diabatic approach of the vibronic coupling theory, and considers a solvent-induced symmetry lowering as a probable mechanism for inducing scattering of totally symmetric motions into a forbidden electronic transition. The second one is based on the theory developed by Korenowski, Ziegler, and Albrecht and assumes that even dipole-forbidden electronic states are possible sources for the Raman-intensity enhancements and for the dispersion of depolarization ratios when a vibrational mixing mode produces vibronic coupling between forbidden and allowed electronic states. Both models seem to be suitable, even if with some differences, for fitting our experimental results for two totally symmetric motions of a soluble form of *cis*-polyacetylene.

I. INTRODUCTION

Depending on whether the polyacetylene chain contains an even or odd number of double bonds, the *cis*-polyacetylene (*cis*-PA) molecule can belong to the C_{2h} or C_{2v} point group of symmetry. Regardless of these structural differences, the absorption spectrum of *cis*-PA reveals a very strong $B \leftarrow A$ transition (at ca. 600 nm) associated with the single-electron π-π^* transition in the π system. On the other hand, the luminescence spectra of *cis*-PA reveal the presence of emission from a weak and short-living state, located at ca. 636 nm above the ground state.[1]

Most experimental data so far available have suggested that the emitting state corresponds to the symmetry-forbidden state of A_g or A_2 symmetry. The close proximity of the strongly allowed B_u (B_1) state and that of the forbidden one may have noticeable consequences for resonant Raman scattering (RRS) if this latter state becomes allowed via mechanisms such as solvent-induced lowering of C_{2h} (C_{2v}) symmetry.[2,3]

The solvent-induced effect of symmetry lowering is based on the observation that the electronic states $\overline{\Phi}^0_m, \overline{\Phi}^0_n, \ldots$ (diabatic approximation) of the isolated molecule can be electronically mixed via interaction with the solvent (environment). The results of this mixing may be such that the "real" electronic states $\Phi^0_m, \Phi^0_n, \ldots$ of the molecule in solution can be approximated as

$$\Phi^0_i = \sum_j C_{ij} \overline{\Phi}^0_j , \tag{1}$$

where the expansion coefficients reflect the solvent (environment)–molecule interaction. If the molecule is placed in an anisotropic environment, and the interaction is not strong, one can expect that the medium will modify predominantly the electronic structure of molecules, leaving their geometrical structure unchanged. In such a case, the forbidden (or very weak) states can borrow intensity from the allowed transitions through the solvent-molecule interaction. It should be noted that the electronic functions Φ^0_i diagonalize the total (solvent-molecule) Hamiltonian with respect to the solvent-molecule interaction. These functions, however, are not the eigenfunctions of the molecular Hamiltonian of the isolated molecule. This implies that the electronic states Φ^0_i can be adiabatically coupled via any kind of vibrational modes, which transform according to the irreducible representation of the point group of the Hamiltonian of the isolated molecule.

The influence of a solvent on the RRS of the metallophthalocyanines was reported a number of years ago.[4] More recently Henneker, Siebrand, and Zgierski[3] have shown that the irregularities observed in the emission and the absorption spectra for $1B_u \leftarrow 1A_g$ and $1A_g \leftarrow 2A_g$ transitions in the octatetracene are due to solvent-induced mixing between $2A_g$ and $1B_u$ states. Since the octatetracene studied earlier[2,3] contains a conjugated double-bond system, as *cis*-PA does, there is reason to suppose that the solvent-induced effect will affect the spectral properties of *cis*-polyacetylene as well.

A quite different way of reasoning can be that based on the theory developed by Korenowski, Ziegler, and Albrecht (KZA).[5] Under this last approach, which is essentially of vibronic character (isolated molecule), appropri-

ate nuclear displacements may induce a vanishing transition dipole moment to be made nonvanishing. This effect is based on the assumption that a displacement along one particular normal coordinate results effectively in making allowed a forbidden electronic transition, with sufficient change in the potential-energy surface, and requires that a Raman-active mode and an electronic mixing mode enter the excited electronic state with a high number of vibrational quanta.

In a previous article,[6] some of us described an interpretation of the experimental Raman excitation profiles (REP's) of a soluble form of *cis*-PA using such solid-state concepts as the band model in metals. The purpose of the present article is, instead, that of showing how the two models depicted above, and described in quantitative detail in the next section, can be applied to the interpretation of the experimental REP's and depolarization dispersion curves of the three resonance-enhanced vibrational motions of this molecule.

II. MODEL FORMULATION

A. Solvent-induced molecular symmetry lowering

For the purpose of this paper we formulate a first model using the representation of Φ_i^0 states defined by Eq. (1), but we will use the notation of the C_{2v} point group throughout this paper. To keep the presentation on the simplest level we will assume that two electronic states $2A_2$ and $1B_1$ of the *cis*-PA molecule contribute to RRS in the excitation region accessible in the current experiments. These two states are correlated to the $2A_g$ and $1B_u$ states when the *cis*-PA has the symmetry of the C_{2h} point group. For practical purposes, we will work in the diabatic approach, in the framework of which the electronic states $2A_2$ and $1B_1$ are represented, respectively, by the electronic functions Φ_m^0 and Φ_n^0 given in the ground-state nuclear equilibrium configuration of the isolated molecule. In this representation, the proximity of the $2A_2$ and $1B_1$ states causes their vibrational manifolds to be involved in both adiabatic and nonadiabatic couplings; to deal with these couplings in a single logical scheme, we will apply already formulated models[7–9] which allow the solution of the vibronic coupling problem by numerical methods. Thus, following that model, the vibronic functions of our two-state approach, which serve as the intermediate states in the RRS process, can be written as

$$\Psi_\nu=\Phi_m^0\xi_\nu^{(m)}+\Phi_n^0\xi_\nu^{(n)} , \tag{2}$$

where the index ν numbers the levels of the excited-state vibronic manifold and the vibrational components $\xi_\nu^{(m)}$ and $\xi_\nu^{(n)}$ can be obtained as solutions of the Schrödinger-like equation

$$\begin{bmatrix} H_{mm} & H_{mn} \\ H_{nm} & H_{nn} \end{bmatrix} \begin{bmatrix} \xi_\nu^{(m)} \\ \xi_\nu^{(n)} \end{bmatrix} = \epsilon_\nu \begin{bmatrix} \xi_\nu^{(m)} \\ \xi_\nu^{(n)} \end{bmatrix} \tag{3}$$

derivable from the variational principle.

For the purposes of presenting the model we will assume that the vibrational manifolds of $2A_2$ and $1B_1$ excited states are each represented by two-dimensional harmonic potentials corresponding to totally symmetric modes which are displaced (not distorted) relative to the ground-state potential. This amounts to the assumption that the diagonal matrix elements in Eq. (3) can be written as[3]

$$\begin{aligned} H_{mm}&=h^0+B_{m1}Q_1+B_{m2}Q_2+E_m^0 , \\ H_{nn}&=h^0+B_{n1}Q_1+B_{n2}Q_2+E_n^0 , \end{aligned} \tag{4a}$$

where B_{mi} and B_{ni} are the Franck-Condon (FC) parameters of the mode in the mth and nth states, respectively. h^0 is the ground-state vibrational Hamiltonian

$$h^0=\tfrac{1}{2}\sum_{i=1,2}(P_i^2+\omega_i^2Q_i^2) . \tag{4b}$$

The off-diagonal matrix element (we assume for simplicity that $H_{nm}=H_{mn}$) in Eq. (3) is responsible for the solvent-induced mixing effect and can be written as[3]

$$H_{mn}=\tau_1Q_1+\tau_2Q_2 , \tag{5}$$

where τ_i $(i=1,2)$ are constants characterizing the interaction between solvent and molecule. When this interaction becomes negligible, both τ_1 and τ_2 vanish as the $2A_2$ and $1B_1$ states cannot be coupled via the totally symmetric vibrations in *cis*-PA with C_{2v} symmetry. It should be noted that the matrix element[7] differs from that given earlier[3] owing to the absence of the constant term (δ_{ab} in Ref. 3). The interaction induced by that term is inherently included in our considerations because of the choice of the $\{\Phi_i^0\}$ representation instead of the $\{\bar{\Phi}_i^0\}$ representation [see the discussion following Eq. (1)].

Within the model sketched above, the RRS tensor can be readily constructed in the condition of resonance with $\Psi_\nu \leftarrow \Psi_0$ vibronic transitions. Hence, if the dipole moments for $\Phi_m^0(B_1)\leftarrow\Phi_0(A_1)$ and $\Phi_n^0(A_2)\leftarrow\Phi_0(A_1)$ electronic transitions are weakly dependent on the vibrational coordinate, and they are oriented as shown in Fig. 1(a), the scattering tensor has the form

$$\{\alpha\}=\begin{bmatrix} \alpha_{xx} & 0 & \alpha_{xz} \\ 0 & 0 & 0 \\ \alpha_{zx} & 0 & \alpha_{zz} \end{bmatrix} . \tag{6}$$

The tensor element $\alpha_{\sigma\rho}$ can be evaluated from[10]

$$\alpha_{\sigma\rho}^{i\rightarrow f}=\sum_\nu \frac{\langle\Psi_f|M_\sigma|\Psi_\nu\rangle\langle\Psi_\nu|M_\rho|\Psi_0\rangle}{\epsilon_\nu-\epsilon_{00}-\Omega-i\Gamma} , \tag{7}$$

where Ψ_f and Ψ_0 represent the final and initial states in the RRS process. The other symbols in (7) have their usual meanings.[11]

Within the formalism outlined above, the excitation profile $\theta(\Omega)$ and depolarization dispersion $\rho(\Omega)$ can be calculated straightforwardly by use of the standard formulas[12]

$$\theta(\Omega)\approx 7|\alpha_{xx}|^2+7|\alpha_{zz}|^2+|\alpha_{xx}+\alpha_{zz}|^2 \tag{8a}$$

and

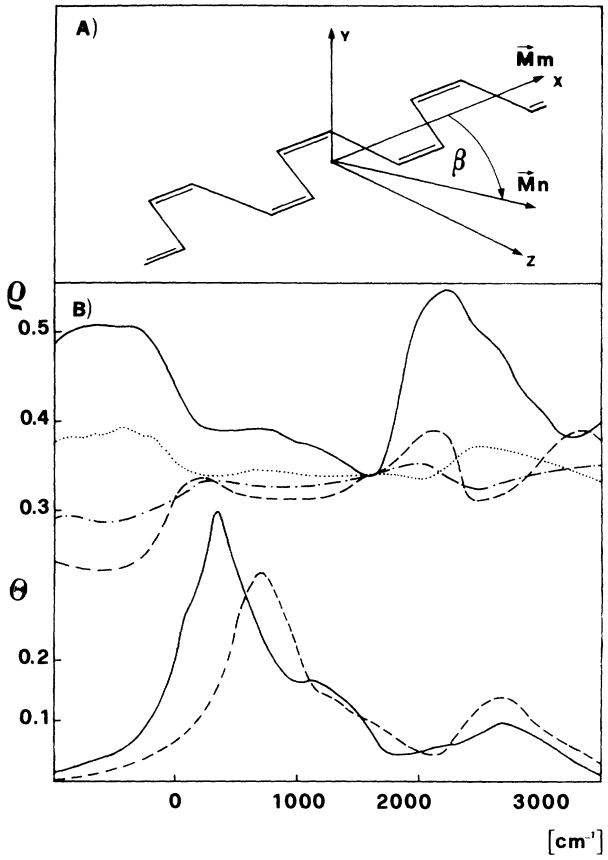

FIG. 1. (a) The fragment of *cis*-PA chain with the possible orientation of transition dipole moments for $B_2 \leftarrow A_1$ ($\bar{M}_m$) and $A_2 \leftarrow A_1$ ($\bar{M}_n$) transitions. (b) The DD (upper curves) and REP (lower curves) for the vibration ω_2 at frequency 1250 cm^{-1}. The second mode is ω_1 at frequency 1540 cm^{-1}. The vibrational parameters used to simulate REP and DD curves are (dimensionless units) $\bar{B}_{n2}=-1.5$, $M_n/M_m=0.5$ (solid lines); $\bar{B}_{n2}=+1.5$, $M_n/M_m=0.5$ (dashed lines); $\bar{B}_{n2}=-1.5$, $M_n/M_m=0.3$ (dotted lines); $\bar{B}_{n2}=+1.5$, $M_n/M_m=0.3$ (dot-dashed lines). The other parameters used in the calculation are listed in Table I.

$$\rho(\Omega)\approx\frac{3|\alpha_{xx}|^2+3|\alpha_{zz}|^2-|\alpha_{xx}+\alpha_{zz}|^2}{4|\alpha_{xx}|^2+4|\alpha_{zz}|^2+2|\alpha_{xx}+\alpha_{zz}|^2} \tag{8b}$$

applicable for randomly oriented molecules. For completeness of this model the inhomogeneous broadening[9] we also included in our calculations. The results of these calculations are presented in Figs. 2 and 3 and discussed in Sec. IV.

TABLE I. Parameters used in Fig. 1(b).

Parameters	mth state	mth state
Γ (cm^{-1})[a]	240	240
Δ (cm^{-1})[b]	100	100
$E_i^0-E_m^0$ (cm^{-1})[c]	0	500
$\bar{B}_1$[d]	0.8	−1.0
$\bar{B}_2$[d]	1.0	

[a]Homogeneous broadening.
[b]Inhomogeneous broadening.
[c]Vertical energy gap referred to the ground-state geometry.
[d]$\bar{B}_i$ is the displacement parameter for the ω_i mode.
[e]Transition dipole moment in the ith direction.

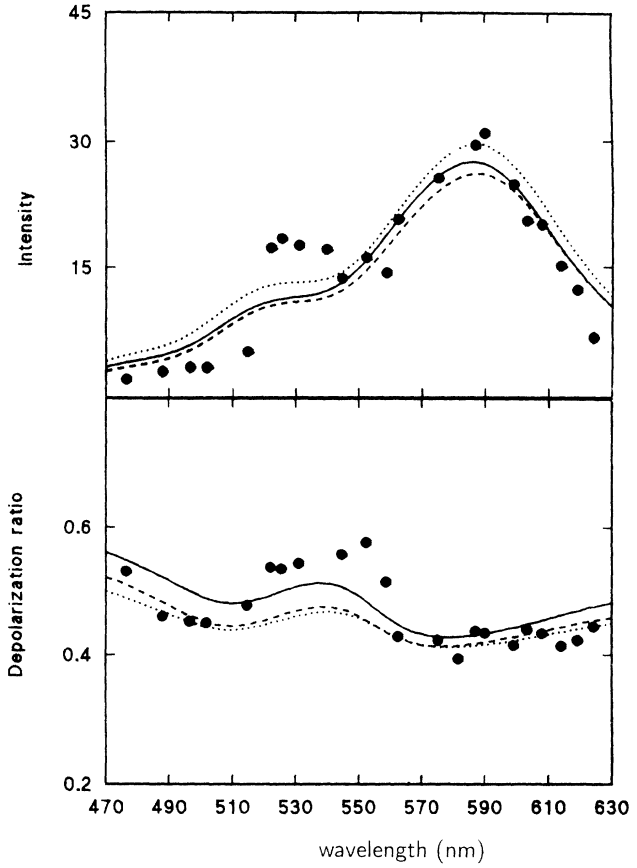

FIG. 2. Comparison between experiment (circles) and theoretical model (lines) for vibrations at 1250 cm^{-1}, adopting the model of the solvent-induced lowering of symmetry. The intensity is in arbitrary units. The parameters used in the calculation are $\bar{\tau}_2=-0.3$ (solid line); $\bar{\tau}_2=0.0$ (dashed line); $\bar{\tau}_2=+0.3$ (dotted line). For the other parameters, see Table II.

B. Using the KZA model

It has been established by Korenowski, Ziegler, and Albrecht[5] that totally symmetric motions may have noticeable scattering intensities and dispersion of depolariza-

TABLE II. Parameters used in Figs. 2 and 3.

Parameter	mth state	nth state
Γ (cm^{-1})[a]	700	700
Δ (cm^{-1})[b]	300	300
$E_i^0-E_m^0$ (cm^{-1})[c]	0	700
$\bar{B}_1$[d]	0.8	−1.0
$\bar{B}_2$[d]	0.9	−1.5
M_i[e]	1.0	0.5

[a]Homogeneous broadening.
[b]Inhomogeneous broadening.
[c]Vertical energy gap referred to the ground-state geometry.
[d]$\bar{B}_i$ is the displacement parameter for the ω_i mode.
[e]Transition dipole moment in the ith direction.

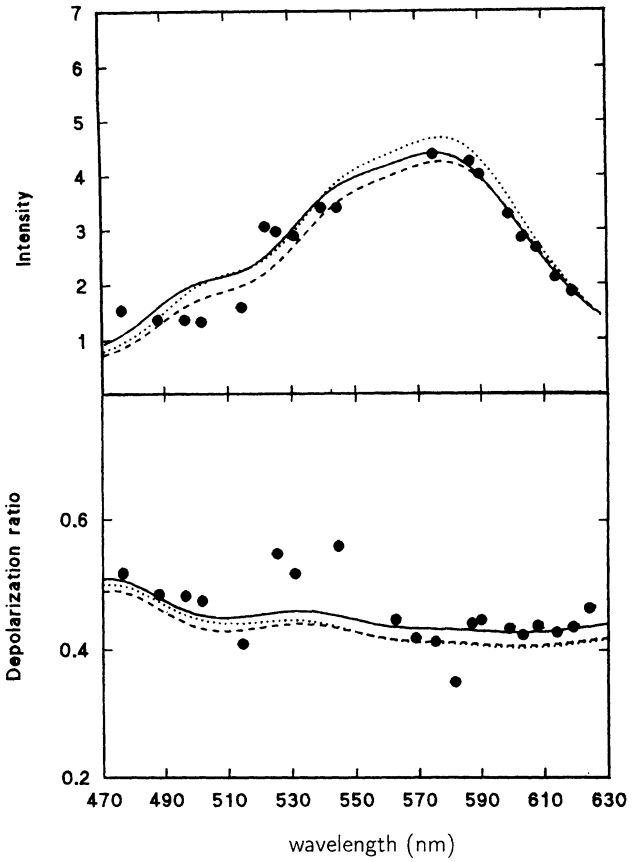

FIG. 3. Same as Fig. 2 for the ω_1 mode at 1540 cm^{-1}.

tion ratios in the excitation range of an electric-dipole-forbidden electronic transition, if vibronic coupling mechanisms are active in mixing the forbidden state with an allowed one, even if the latter lies completely off-resonance. The theory and the relevant equations have been exhaustively described in Ref. 5 and are not therefore reported here, except those giving the final expressions necessary to calculate, in the framework of this model, the REP cross sections and the depolarization dispersion (DD) curves. These are

$$(\alpha^{A_2})_{0,1}=D_{A_2}\sum_{v_r}\langle 0|v_r\rangle\langle v_r|1\rangle \times\int\frac{g(\bar{\nu}_{v'})d\bar{\nu}_{v'}}{(\bar{\nu}_{v'}+\bar{\nu}_{v_r}+\bar{\nu}_{v_a}+\bar{\nu}_e^0)-\bar{\nu}_0+i\Gamma_e}\ , \tag{9}$$

TABLE III. Parameters used in Figs. 4 and 5.

Parameter	mth state	nth state
Δ (cm^{-1})[a]	100	100
$E_i^0-E_m^0$ (cm^{-1})[b]	0	700
$\bar{B}_1$[c]	0.6	1.2
$\bar{B}_2$[c]	0.4	1.0
M_i[d]	1.0	0.65

[a]Inhomogeneous broadening.
[b]Vertical energy gap referred to the ground-state geometry.
[c]$\bar{B}_1$ is the displacement parameter for the ω_i mode.
[d]Transition dipole moment in the ith direction.

$$\rho_n(\bar{\nu}_0)=\frac{2(2\delta-\gamma)}{8\delta+\gamma}\ . \tag{10}$$

As the reader can see, Eqs. (9) and (10) correspond to Eqs. (4) and (6) in Ref. 5, with the necessary modifications due to the different molecules and transitions treated in the two cases.

In particular, the A_2 electronic band of *cis*-PA can consist of false origins arising from vibrations of species a_2 (for polarization along z), b_2 (polarization along x), and b_1 (polarization along y). Due to the fact that the B_1 allowed band is very close to the forbidden A_2 one, the b_2 false origins should presumably dominate. Thus, the false-origin spectrum, which contributes to the whole A_2 band, will scatter totally symmetric motions resonantly as a fully allowed band does. Of course, each false-origin subband contributes to the scattering with its own isotropic element of the polarizability tensor, i.e., α_{zz} for a_2, α_{xx} for b_2, and α_{yy} for b_1 motions, respectively. This mechanism in the A_2 transition can lead both to polarization dispersion and to complicated aspect in the REP's. Moreover, these A_2 state polarizabilities will produce interference with channels from different nonresonant states, certainly with those arising from the near-lying B_1 intense band. Thus, if we assume that the scattering from the $^1B_{2u}$ forbidden transition in benzene, described in Ref. 5, can be viewed as a mechanism analogous to that observed in the present case, these interferences can lead to dispersion in the depolarization ratio values and to complicated shapes of the excitation profiles, even if only one false-origin band dominates the A_2 forbidden transition. The main advantage in the use of this approach lies in the fact that, using a large number of FC integrals, i.e., many vibrational quanta of the intermediate state, we do not need to introduce very large values of the homogeneous and inhomogeneous broadening when fitting the experimental points.

Fittings of the experimental points of the REP's and DD curves are reported in Figs. 4 and 5 with the use of this second approach. A comparison between the two models outlined above is discussed below. However, as can be seen by comparing Fig. 2 with Fig. 4 (ω_2 mode at 1250 cm^{-1}) and Fig. 3 with Fig. 5 (ω_1 mode at 1540 cm^{-1}), whilst the agreement between experimental points and computed curves is not appreciably dependent on the model used as far as the REP's are concerned, noticeable differences can be observed in the case of the DD curves, for which the KZA model seems to produce worse results.

III. EXPERIMENTAL

The soluble sample of *cis*-PA was prepared at the ICM-NRC laboratories (Milan), by inserting chains of PA on a long chain of polybutadiene in order to solubilize the polymer. The distribution length of *cis* chains was estimated, by the uv spectrum, to be 12–14 C atoms. In the final product about 40% of *trans*-PA is retained in the copolymer, but this does not disturb the band-area measurements of RR lines of *cis*-PA.

The solvent utilized in recording the spectra was

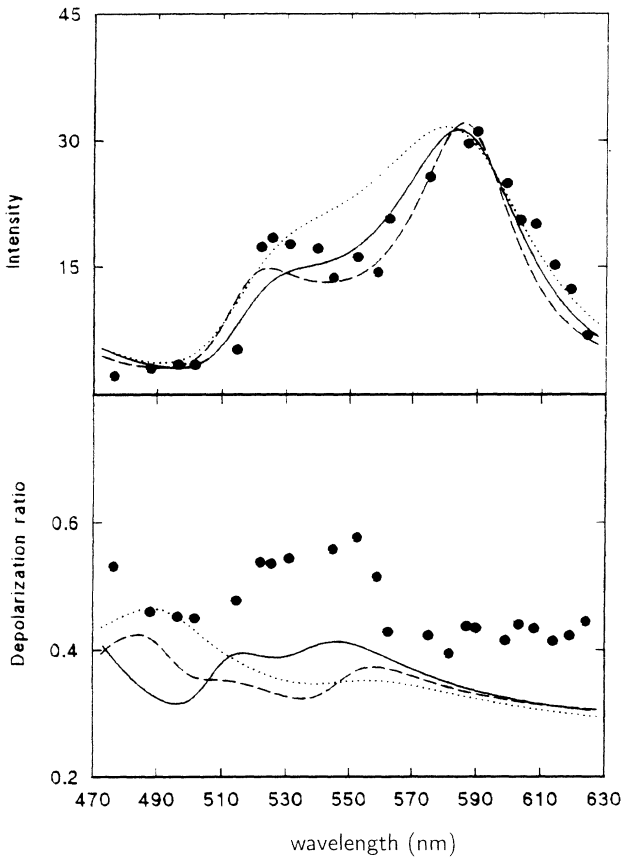

FIG. 4. Comparison between experiment (circles) and theoretical model (lines) for vibrations at 1250 cm^{-1}, in the KZA approach. The parameters used in the calculation are $\Gamma=300$ cm^{-1} (solid line); $\Gamma=200$ cm^{-1} (dashed line); $\Gamma=400$ cm^{-1} (dotted line). For the other parameters, see Table III.

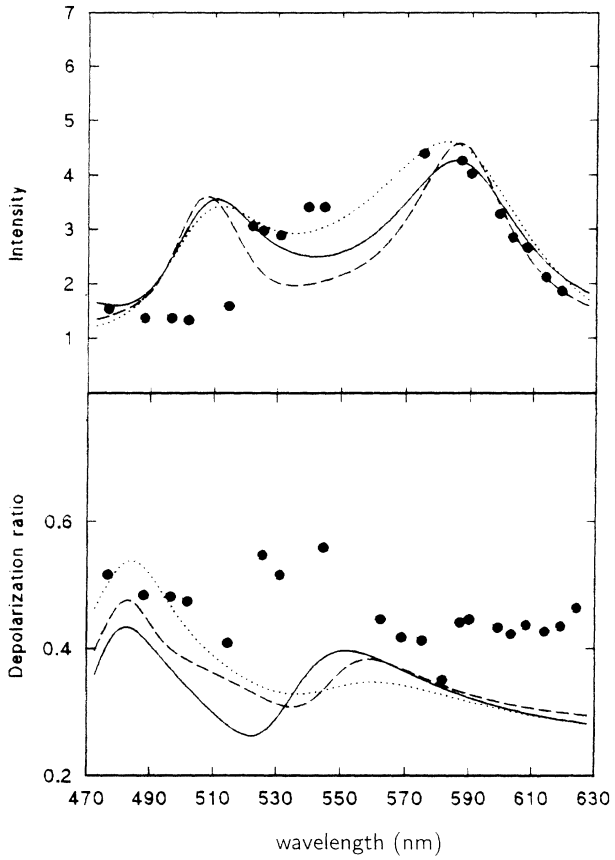

FIG. 5. Same as Fig. 4 for the ω_1 mode at 1540 cm^{-1}.

spectroscopic-grade toluene. For the evaluation of absolute intensities of RR lines, we selected the 1210 cm^{-1} Raman line of toluene, which was used as internal standard. The stability of the solutions was always checked by a visible spectrum recorded immediately before each run of the RR spectra, at the different excitation wavelengths.

Visible spectra were obtained with a Lambda 5 Perkin-Elmer uv-Vis spectrometer, using solutions of approximate concentration $5\times10^{-2}M$. The RR spectra were measured in a 90° scattering geometry; the scattered light was detected with a Jobin-Yvon Ramanor HG 2S holographic grating double monochromator, equipped with a thermoelectrically cooled Hamamatsu 943XX phototube and a photon-counting system. The signal was processed through the Jobin-Yvon "enhanced PRISMA" software package, which is used for the acquisition and treatment of raw experimental data. Each measured intensity comes from an averaging procedure done on at least ten recordings. Excitation wavelengths were obtained by a Coherent Innova 400/10 cw argon-ion laser and by Spectra Physics Model 375 cumarine 6 and rhodamine 6G tunable dye lasers.

Depolarization ratios (ρ) of the three lines of *cis*-PA were measured with standard polaroids, scrambling the scattered radiation to take into account the different sensitivity of gratings to I_{VV} and I_{VH} detection. Band areas of deconvoluted and smoothed Raman lines were used as experimental points.

IV. RESULTS AND DISCUSSION

In this section we want to present and discuss the results of our calculations executed by using both the models sketched in Secs. II A and II B. The first part concerns the use of the solvent-induced mechanism of molecular symmetry lowering; the second one regards the calculations made in the frame of the KZA theory.

Figure 1(b) shows excitation profile and depolarization curves calculated for the vibrational mode ω_2 at 1250 cm^{-1} and B_{ki} and τ_i parameters which, expressed in dimensionless units ($\tilde{B}_{ki}=B_{ki}\omega_i^{-3/2}$, $\tilde{\tau}=\tau_i\omega_i^{-1/2}$), are $\tilde{B}_{m2}=1$, $\tilde{B}_{n2}=\pm1.5$, and $\tilde{\tau}_2=-0.3$. For the second mode ω_1 at 1540 cm^{-1} the relevant parameters are $\tilde{B}_{m1}=0.8$, $\tilde{B}_{n1}=-1.0$ and $\tilde{\tau}_1=0$. These parameters are very close to those expected for a molecule like *cis*-PA. The solid and dashed curves in Fig. 1(b) correspond to the situation when $\tilde{B}_{m2}$ is constant but the FC parameter in the nth state has a different sign. The dotted and dash-dotted lines in Fig. 1(b) correspond to the solid and dashed lines of the DD, respectively, but these were obtained for a smaller value of the ratio M_n/M_m. In this case, the influence of the nth state is smaller.

Figure 1(b) also shows that the values of ρ reported by Lanzani *et al.*[13] can easily be reached within the model formulated. The range of variability of ρ for the vibrations measured by us is in good agreement with that predicted by the model, and offers evidence for a pronounced dispersion of the polarization.

Negative values of $\tilde{B}_{n2}$ and $\tilde{\tau}_2$ are consistent with the diabatic approach we adopted for the representation of crossing potential-energy surfaces of the excited states; such a situation was found to have physical meaning in the quantitative description of absorption and RR scattering of long-chain polyenes.[3,11]

As can be seen from Fig. 1(b), both the REP and the DD curves show a rather complex behavior in the entire excitation region. This was expected because two overlapping states give rise to RRS and strong interference effects can occur. In the excitation profiles these interferences are manifested in a pronounced fashion in the low-energy part of the REP, where the interferences give rise to the significant blueshift of the REP when $\tilde{B}_{ni}$ changes sign. Such a behavior can easily be understood in terms of a single-mode approach,[9] applied in the absence of the solvent-induced effect (i.e., when $\tilde{\tau}_1=\tilde{\tau}_2=0$) and in the case where the inhomogeneous broadening is negligible. In such a case, the tensor elements α_{xx} and α_{zz}, calculated in the vicinity of the lowest-energy transitions, can be approximated by

$$\alpha_{xx}=\sum_v \frac{(1|\bar{v}_m)(\bar{v}_m|0)}{E_m^0-\Omega-i\Gamma}M_m^2 ,$$
$$\alpha_{zz}=\sum_v \frac{(1|\bar{v}_n)(\bar{v}_n|0)}{E_n^0-\Omega-i\Gamma}M_n^2 , \tag{11}$$

where

$$(1|\bar{0}_k)(\bar{0}_k|0)=-\frac{\sqrt{2}}{2}B_{ki}e^{-(1/2)B_{ki}^2} .$$

Since the condition $M_n^2/M_m^2 \ll 1$ holds in our calculations, the strong change in intensity distribution observed in the low-energy part of the REP is due to the modulation of the $|\alpha_{xx}+\alpha_{zz}|^2$ term in Eq. (8a). Expressions (11) show that the changes of these terms should be large on going from a positive value of B_{n1} to a negative one. These changes are accompanied by substantial changes of the depolarization dispersion curves in the preresonance excitation region, as shown in Fig. 1(b).

Although the model formulated in this paper is very simple, it is interesting to test how it works if applied to a real molecule such as *cis*-PA. Figure 2 shows the comparison between experimental and theoretical REP and DD for the vibrational mode with frequency $\omega_2=1250$ cm^{-1}. The relevant parameters $\tilde{B}$ and $\tilde{\tau}$ were adjusted by a trial and error procedure but the angle β [Fig. 1(a)] was arbitrarily fixed to be 70°. Figure 3 shows the results of a similar calculation performed for the vibrational mode with frequency $\omega_1=1540$ cm^{-1}.

The vertical energy gap for the ground-state geometry, $E_n^0-E_m^0=700$ cm^{-1}, was chosen somewhat arbitrarily but, for the FC parameters used in these calculations, the set of parameters locates the bottom of the potential surface of the nth state to be lower in energy than its counterpart in the mth state. Thus, in agreement with experiment, the emission will occur from the less intense state (A_2) located at a lower energy than that of the intense (B_1) one. The absorption spectrum, calculated with the parameters used here, also agrees with the expected absorption.

As can be seen from Figs. 2 and 3 the agreement between our model and experiments is quite striking, even if the parameters used in the calculations have only an approximate value. In fact, the change of the parameter τ from positive to negative values (the zero value indicates that vibronic coupling between the two states is assumed to be absent) seems to be more effective in the case of the DD curves, especially for the low-energy excitation region, than for the REP's; in this latter case, the best fit appears instead to be strongly dependent on a consistent value of the inhomogeneous broadening parameter which, in turn, takes account of the degree of interaction between the molecule and its environment.

Although refinement is always possible in the present model, the agreement with experiment, as it stands, provides a strong indication that the A_2 state is implied. This state, through the solvent-induced effect of symmetry lowering, enters the RRS spectrum in the region of the strong $B_1 \leftarrow A_1$ electronic transition in *cis*-polyacetylene.

Similar results to those obtained for the vibrational motions ω_2 and ω_1 can also be obtained for the ω_3 mode at 910 cm^{-1}. The calculation for the latter motion is not included in the present paper because we have not been successful in reproducing a reasonably good fit of the DD curve and, on the other hand, as far as the REP is concerned, we have already presented the results,[6] even if from a different point of view.

We want to shift our attention now to the results obtained with the KZA model. In the framework of this approach, we have executed calculations in which the displaced harmonic-oscillator wave functions were used as bases and the adjustable values were the vibrational displacement parameters, the energy gap between excited electronic states, the transition moment values, and the orientation of the relevant vectors, besides the number of vibrational quanta involved in the excited-state manifold (number of FC integrals).

As regards the damping-constant values, we used, even in this case, two different numbers in order to separate the contribution due to the natural lifetime of the vibronic states from that due to environmental effects (inhomogeneous broadening). In particular, we have adopted values of homogeneous and inhomogeneous broadening which are considered quite standard in systems like these.[6,14,15] As described in Ref. 5, the main advantage in the use of the KZA model is that the numerical reproduction of experimental points can easily be reached with much smaller values of the damping constants: $\Gamma=300$ cm^{-1} (± 100 cm^{-1}) and $\Delta=100$ cm^{-1}.

Looking at Figs. 4 and 5 we can observe that, although the shape of the DD curves is in good agreement with the pattern given by the experimental points, the curves obtained with the three different sets of parameters do not

correctly fit their numerical values as the previous model does.

V. CONCLUSIONS

The two models we have used to calculate REP's and DD curves which could fit experimental RR results concerning two totally symmetric motions of soluble *cis*-PA give rise to a different degree of agreement with the experiments, if the relevant theories are "pushed" to the same level of approximation. Without doubt the KZA approach gives us the possibility of using an elegant and flexible model which, moreover, seems to be very useful when many of the $3N-6$ normal modes of a molecule are handled all together, and more than two electronic states in resonance and out of resonance are considered. In addition, the summation over many vibrational quanta of the excited state (large values of displacement parameters) will fit the experimental points without the necessity of introducing large (often unphysical) damping constants. In our case, where only two normal motions of *cis*-PA have been considered, the two models used give quite comparable results as far as the REP's are concerned but, as the figures here indicate, the solvent-induced symmetry lowering approach seems to be more suitable when the DD curves should be reproduced. Owing to the fact that the purpose of this paper is mainly that of giving a modelistic interpretation of the dispersion curves of the depolarization ratios of totally symmetric modes of *cis*-PA that we have observed experimentally, we lean a little more towards the symmetry lowering model which, on the other hand, cannot be considered definitely favored over the vibronic KZA one, if other symptoms of the dominance of the solvent effect are not explored. Among others, these symptoms could be the solvent dependence of absorption polarization within the A_2 band, the solvent dependence of A_2 fluorescence yields, and the solvent dependence of the REP's and the DD curves.

In conclusion, in the framework of vibronic coupling theory, our nonadiabatic approach for the electronic excitation treatment of *cis*-PA leads to a good fit of the experimental RR excitation profiles of the three totally symmetric motions of the molecule in solution. The same model also allows us to reproduce quite nicely the dispersion curves of the depolarization ratio of two of these modes over a large part of the excitation region.

ACKNOWLEDGMENTS

The authors wish to express their sincere thanks to Dr. Silvia Destri at the ICM-NRC laboratories (Milan) for a generous gift of soluble *cis*-PA and useful discussions. Acknowledgment is also due to the Italian Consiglio Nazionale delle Ricerche (Rome), Progetto Finalizzato "Chimica Fine e Secondaria II."

[1]L. S. Lichtmann, E. A. Imhoff, A. Sarhangi, and D. B. Fitchen, J. Chem. Phys. **81**, 168 (1984).

[2]T. Ikeyama and T. Azumi, J. Chem. Phys. **76**, 5672 (1982).

[3]W. H. Henneker, W. Siebrand, and M. Z. Zgierski, J. Chem. Phys. **79**, 2495 (1983).

[4]M. Pawlikowski and M. Z. Zgierski, Chem. Phys. Lett. **74**, 327 (1980).

[5]G. M. Korenowski, L. D. Ziegler, and A. C. Albrecht, J. Chem. Phys. **68**, 1248 (1978).

[6]P. Sassi and R. S. Cataliotti, Mol. Phys. **77**, 937 (1992).

[7]W. H. Henneker, A. Penner, W. Siebrand, and M. Z. Zgierski, J. Chem. Phys. **69**, 1884 (1978).

[8]W. Siebrand and M. Z. Zgierski, J. Chem. Phys. **71**, 3561 (1979).

[9]W. Siebrand and M. Z. Zgierski, in *Excited States,* edited by E. C. Lim (Academic, New York, 1979), Vol. 4, p. 1.

[10]H. C. Longuet-Higgins, Adv. Spectrosc. **2**, 429 (1961).

[11]A. R. Gregory, W. H. Henneker, W. Siebrand, and M. Z. Zgierski, J. Chem. Phys. **63**, 5475 (1975).

[12]O. Sonnich Mortensen and S. Hassing, in *Advances in IR and Raman Spectroscopy,* edited by R. J. H. Clark and R. E. Hester (Heyden, London, 1980), Vol. 6, p. 1.

[13]G. Lanzani, S. Luzzati, R. Tubino, and G. Dellepiane, J. Chem. Phys. **91**, 732 (1989), and papers cited therein.

[14]W. Siebrand and M. Z. Zgierski, J. Chem. Phys. **81**, 185 (1984).

[15](a) R. S. Cataliotti, G. Paliani, G. Dellepiane, S. Fuso, S. Destri, L. Piseri, and R. Tubino, J. Chem. Phys. **82**, 2223 (1985); (b) S. Fuso, C. Cuniberti, P. Piaggio, G. Dellepiane, S. Luzzati, R. Tubino, and M. Z. Zgierski, *ibid.* **87**, 6816 (1987).